Desalination and Water Treatment
www.deswater.com

doi: 10.1080/19443994.2012.762945

51 (2013) 5735–5745
August

Taylor & Francis
Taylor & Francis Group

Biosorption of copper ion by natural and modified wheat straw in fixed-bed column

Yike Li, Binglu Zhao, Lijun Zhang, Runping Han*

School of Chemistry and Molecular Engineering, Zhengzhou University, No. 100 of Kexue Road, Zhengzhou 450001, P.R. China
Tel. +86 371 67781757; Fax: +86 371 67781556; email: rphan67@zzu.edu.cn

Received 1 November 2012; Accepted 26 December 2012

ABSTRACT

Adsorption of copper ions from aqueous solution was studied by natural wheat straw (NWS) and modified wheat straw (MWS) with citric acid in fixed-bed column. The experiments were conducted to investigate the effects of the bed depth, the flow rate, and the influent concentration of copper ions. The column data were fitted by the Thomas model using nonlinear regressive analysis while bed depth/service time analysis (BDST) model was applied at different bed depth. The Thomas model was found suitable for the description of breakthrough curve. The bed depth service time (BDST) model was applied to predict the service times with other flow rate and initial concentration. The theoretical breakthrough curve was compared with experimental breakthrough curve profile in the dynamic process. The copper-loaded adsorbent was regenerated using hydrogen chloride solution. The results showed that the adsorption capacity of MWS for copper ion was higher than NWS and both NWS and MWS can be reused.

Keywords: Wheat straw; Modified wheat straw; Copper ion; Column adsorption; Models

1. Introduction

The removal of heavy metals ions from wastewater has received a great attention for global awareness of the underlying detriment of heavy metals in the environment. Adsorption techniques have proved to be effective and attractive processes for the treatment of heavy metal-bearing wastewaters [1]. Since activated carbon is expensive and regeneration of exhausted carbon is cost, an alternative inexpensive adsorbent can reduce the cost of an adsorption system. Agricultural waste materials are economic and eco-friendly due to their unique chemical composition, availability in abundance, renewable, low in cost and more efficient, and are seem to be viable option for heavy metal remediation [2]. Some of these byproducts such as rice husk, wheat straw, cereal chaff, etc. [3–6] were used to remove metals from solution and several reviews were published [7–10].

As a matter of fact, natural agricultural products directly used as adsorbent are not advantageous for physical and chemical characteristics. Therefore, these materials need to be modified or treated before being applied for the decontamination of heavy metals and other pollutants. Furthermore, modification of agricultural by-products can be carried out to achieve adequate structural durability, enhance their natural ion exchange capability and add value to the by-product. The methods were reviewed [11,12] and some modified adsorbents, such NaOH-treated husk, ethylenediamine-modified rice hull, were used for removal of metal or dye ions from solution [13–15].

*Corresponding author.

In this article, wheat straw was selected as an adsorbent for the removal of copper ions from aqueous solutions because of two factors. Firstly, wheat straw contains adequate cellulose and several functional groups such as hydroxy, carboxyl, and amidogen, making the adsorption processes more feasible [16]. Furthermore, wheat is a widely cultured food crop in China. Consequently, the wheat straw was obtained extensively and cheaply as a byproduct acquired from agriculture. Chemical modification using citric acid (CA) was an effective process to enhance the adsorption capacity of natural wheat straw (NWS) and soybean hulls for metal ions and dyes [16–17].

Previously in our laboratory, NWS- and CA-modified wheat straw (MWS) were used as adsorbents to remove Methylene blue and copper ion from solution in batch mode, respectively [4,16]. However, the information from the batch experiments did not apply to continuous operation. The engineering advantages of a fixed-bed adsorption column with adsorbents offer easy continuous operation and scale up is important of the adsorption process. But no research was reported about copper ions adsorption onto NWS and MWS in column mode. Therefore, it is imperative to describe dynamic behavior in a fixed-bed column condition.

The research described here was designed to investigate the biosorption behavior of NWS and MWS in order to remove copper ions from solution in fixed-bed column. The effects of main variables, such as flow rate, influent concentration, and bed depth on copper ions adsorption were researched. In order to predict the performance in the column, the experimental data were processed with Thomas model and bed depth/service time model. The exhausted NWS and MWS were regenerated using 0.5 mol L^{-1} hydrogen chloride solution and reuse of NWS and MWS was evaluated.

2. Materials and methods

2.1. Preparation of natural wheat straw and modified wheat straw

Fresh biomass of wheat straw was obtained from local countryside of Luoyang City, China. The collected wheat straw was washed with distilled water several times and dried in an oven at 50°C. Dry wheat straw was crushed into powder and screened through a set of sieves (20–40 mesh), which produced a uniform material for the adsorption tests, and then conserved in the desiccator for use.

The preparation process of MWS follows [16]: ground wheat straw was mixed with 0.6 mol L^{-1} CA at the ratio of 1:12 (straw/acid, w/v) and stirred for 30 min at 20°C. The acid straw slurries were placed in a stainless steel tray and dried at 50°C in a forced air oven for 24 h. Then temperature was raised up to 120°C for 90 min. After cooling, the esterified wheat straw was washed with distilled water until the liquid did not turn turbidity when 0.1 mol L^{-1} lead (II) nitrate was dropped in. After filtration, MWS was suspended in 0.1 mol L^{-1} NaOH solution at suitable ratio and stirred for 60 min, followed by washing thoroughly with distilled water to remove residual alkali, next dried at 50°C for 24 h and preserved in a desiccator for use.

2.2. Copper ion solution

Stock solutions of 500 mg L^{-1} Cu(II) were prepared from $CuCl_2$ in distilled, deionized water containing a few drops of concentrated HCl to prevent the precipitation of Cu^{2+} by hydrolysis. All working solutions were prepared by diluting the stock solution with distilled water to the needed concentration and solution pH was adjusted to 4.0.

2.3. Column adsorption studies

Fixed-bed column adsorption experiments were carried out using NWS and MWS packed into a glass column (1.0 cm inner diameter and 25 cm in height) with a bed depth of 6, 8.5, and 11 cm, respectively. The experiments were conducted by pumping copper solution in down flow mode through the fixed-bed with a peristaltic pump. The temperatures of all experiments were 293 K. Samples were collected at regular intervals in the adsorptive process. Copper ion was measured using atomic absorption spectrometry at 234.8 nm (AAanalyst300, Perkin-Elmer).

The concentration of copper ions desorbed from Cu-loaded adsorbents in column by 0.5 mol L^{-1} hydrogen chloride solution was also analyzed and the regenerated column was reused to adsorb copper ions for NWS and MWS (for column depth 8.5 cm, flow rate 5.6 mL min^{-1}, copper ion concentration 20 mg L^{-1}).

3. Result and discussion

3.1. The effect of flow rate on breakthrough curves

The breakthrough curves at various flow rates were shown in Fig. 1.

It was observed that breakthrough generally occurred faster and the breakthrough curve was steeper with higher flow rate for both NWS and MWS, respectively. Breakthrough time reaching saturation was significantly increased with a decreased in the

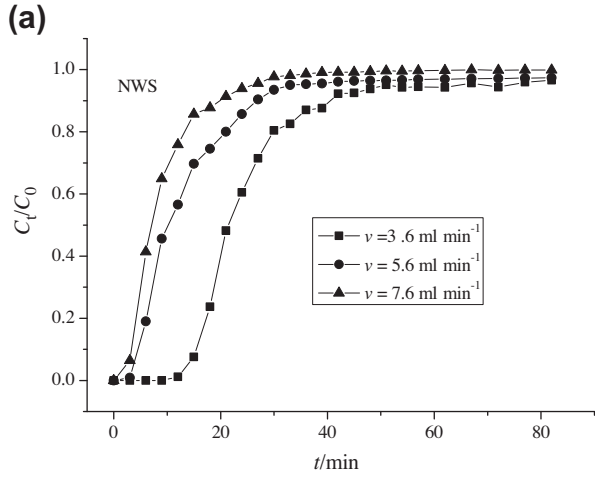

Fig. 1. Breakthrough curves at various flow rate on copper adsorption ($Z = 8.5$ cm, $C_0 = 20$ mg L^{-1}).

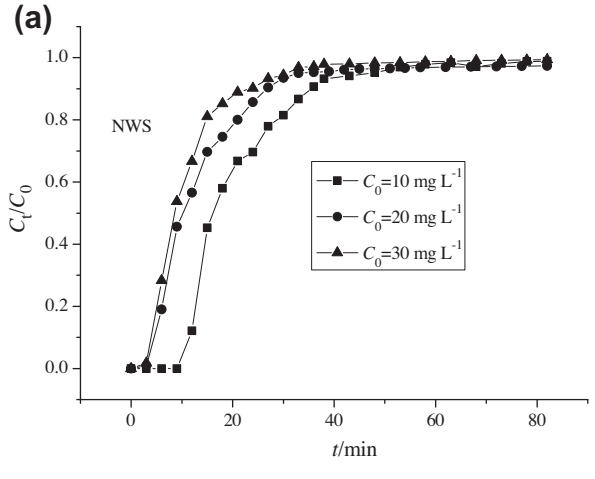

Fig. 2. Breakthrough curves at different influent concentration ($Z = 8.5$ cm, $v = 5.6$ mL min^{-1}).

flow rate. At a low rate of influent, copper ions had more time to contact with adsorbents and this resulted in higher removal of copper ions in column.

3.2. Effect of influent copper ion concentration on breakthrough curves

The effect of influent copper ions concentration on the shape of the breakthrough curves is shown in Fig. 2.

It was shown that the breakthrough time occurred fast with increasing influent copper concentration. Breakthrough curves were dispersed and breakthrough occurred slower at lower influent metal concentrations while sharper breakthrough curves were obtained at higher influent concentration. The larger the influent concentration, the steeper is the slope of breakthrough curve and smaller is the breakthrough time. These results demonstrate that the change of concentration gradient affects the saturation rate and breakthrough time.

3.3. The effect of different bed depth on breakthrough curves

The breakthrough curve at different bed depths for NWS and MWS is shown in Fig. 3, respectively.

From Fig. 3, as the bed height increased, copper ions had more time to contact with adsorbent, resulting in more efficient removal of copper ion. Thus, the higher bed height resulted in a decrease in copper ion concentration in the effluent. The slope of the breakthrough curve decreased with increase in bed height as a result of broadened influent movement zone.

Compared to breakthrough curves (Figs. 1–3) at same condition (same about bed depth, flow rate, and copper concentration) between NWS and MWS, it can be seen that the breakthrough time and exhausted time of MWS are longer than those of NWS, respec-

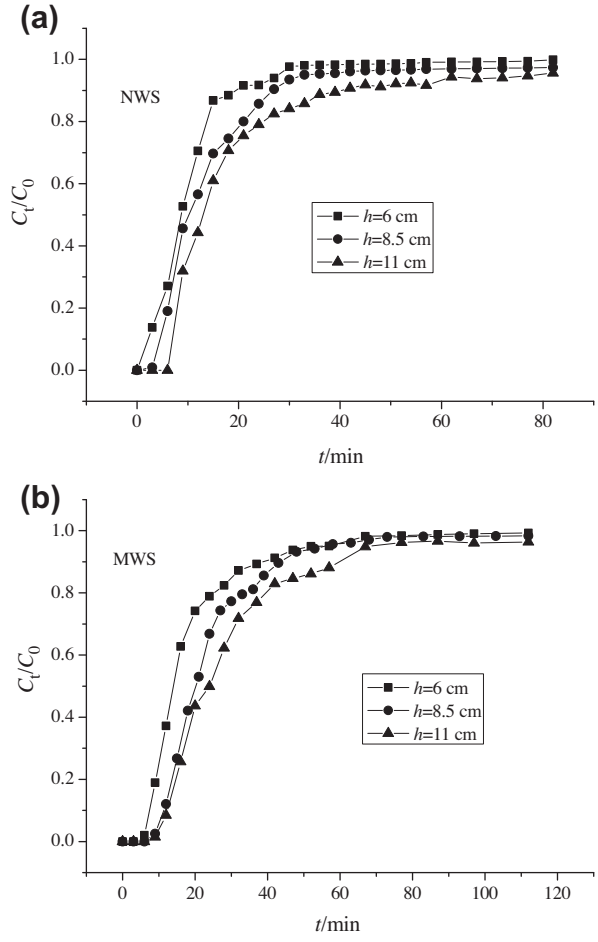

Fig. 3. Breakthrough curves at different bed depths ($C_0 = 20\,mg\,L^{-1}$, $v = 5.6\,mL\,min^{-1}$).

tively. These results showed that MWS had more adsorption capacity for copper ions than NWS. This was also confirmed by adsorption in batch mode [4,16]. The mechanism may be the rough surface and more functional groups (carboxyl groups) made MWS's beneficial to adsorb metal cation ion from solution [16].

3.4. Regeneration and copper-loaded NWS and MWS and reuse

Disposal of the metal-loaded adsorbent creates another environmental problem as it is hazardous material. The use of biomass as a potential adsorbent depends not only on the adsorptive capacity, but also on how well the biomass can be regenerated and reused, especially for modified adsorbents. Regeneration must produce small volume of metal solution without significantly damaging the capacity of the adsorbent, making it reusable in several adsorptions and desorption cycles [18–21].

Fig. 4 shows the desorbed curves using $0.5\,mol\,L^{-1}$ hydrogen chloride solution. As shown in Fig. 4, copper ion was easily desorbed because the desorption nearly completed in less than 10 min. Fig. 5 shows the recycles of copper ions adsorbed by NWS and MWS. The first, second, and third regeneration yields are 88.1, 57.8, and 57.0% for NWS and 75.3, 48.8, and 44.3% for MWS, respectively. The results showed that NWS and MWS can be used repeatedly with losing some adsorption capacity for removal of copper ions from solution (Fig. 5).

3.5. Modeling of column study

3.5.1. Thomas model

The Thomas model is used to calculate the maximum solid phase concentration on adsorbent and the adsorption rate constant. The expression by Thomas for an adsorption column is given as follows [22]:

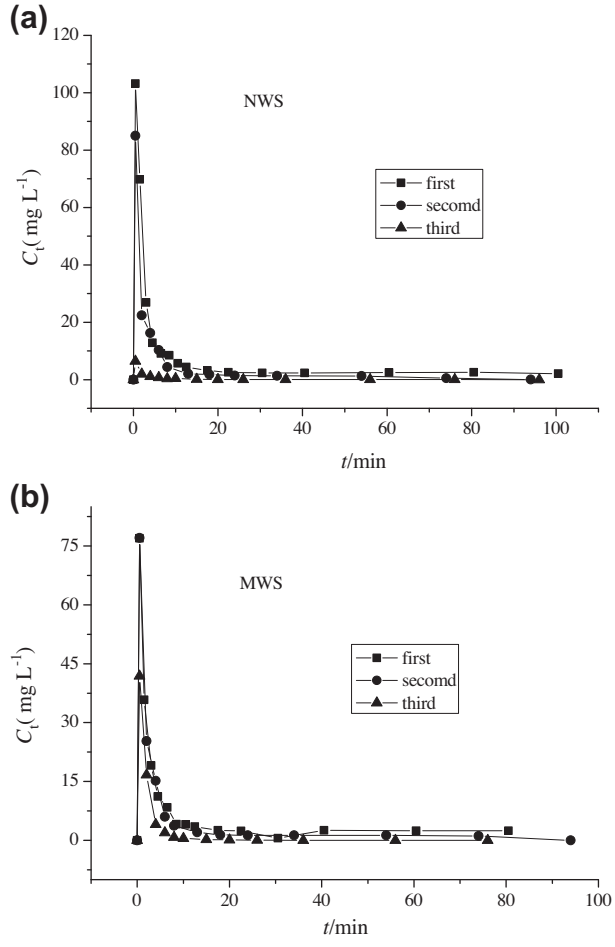

Fig. 4. Elution curves for copper ions from NWS and MWS column using $0.5\,mol\,L^{-1}$ HCl solution ($Z = 8.5\,cm$, $C_0 = 20\,mg\,L^{-1}$, $v = 5.6\,mL\,min^{-1}$).

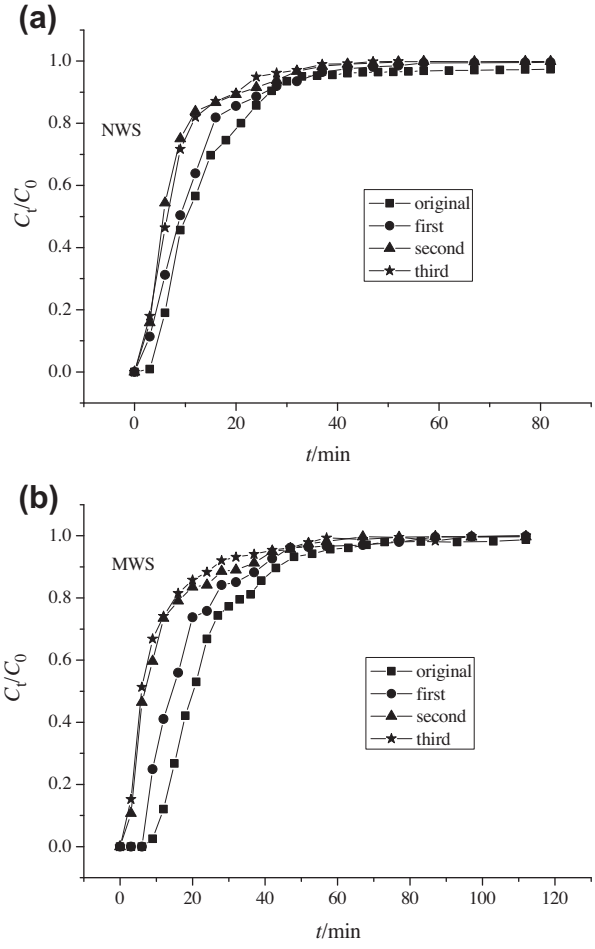

Fig. 5. Adsorption/desorption recycles about copper ions adsorption onto NWS and MWS columns ($Z = 8.5$ cm, $C_0 = 20\,\mathrm{mg\,L^{-1}}$, $v = 5.6\,\mathrm{mL\,min^{-1}}$).

$$\frac{C_t}{C_0} = \frac{1}{1 + \exp(k_{Th} q_0 x/v - k_{Th} C_0 t)} \quad (1)$$

where q_0 is the adsorption capacity per g of the adsorbent ($\mathrm{mg\,g^{-1}}$); k_{Th} is the rate constant ($\mathrm{mL\,min^{-1}\,mg^{-1}}$); x is the quantity of adsorbent in the column (g); C_0 is the influent copper ion concentration ($\mathrm{mg\,L^{-1}}$); C_t is the effluent concentration at any time t ($\mathrm{mg\,L^{-1}}$); and v is the flow rate ($\mathrm{mL\,min^{-1}}$). The value of C_t/C_0 is the proportion of effluent and influent copper ion concentration.

From a plot of C_t/C_0 against t at a given flow rate using nonlinear regression, A ($k_{Th} q_0 x/v$) and B ($k_{Th} C_0$) can be obtained. As values of initial concentration C_0, adsorbent mass x and flow rate v are known, the kinetic coefficient k_{Th} (from B) and the adsorption capacity of the column q_0 can be calculated. The parameters of Thomas model are listed in Table 1. Values of error (x^2) and q_{exp} (from experiment) are also listed in Table 1.

From Table 1, with flow rate increasing, the value of q_0 for NWS and MWS decreased but the value of k_{Th} increased. As the bed depth increased, the value of q_0 and k_{Th} decreased for two adsorbents. With the increase in copper ion concentration, values of q_0 increased but it was opposite to values of k_{Th}. It was also obtained that the adsorption capacity of MWS was larger than that NWS from Table 1.

They were all with higher determined coefficients (R^2) (larger 0.96) and lower x^2 (smaller than 0.00800) from Table 1. But the value of q_0 is not close to q_{exp} at same condition. So it was concluded that Thomas model be suitable to fit experimental data.

3.5.2 The Yoon–Nelson model

The Yoon–Nelson model not only is less complicated than other models, but also requires no detailed data concerning the characteristics of adsorbate, the type of adsorbent, and the physical properties of adsorption bed. The Yoon–Nelson equation regarding to a single component system is expressed as [23]:

$$\frac{C_t}{C_0 - C_t} = \exp(k_{YN} t - \tau k_{YN}) \quad (2)$$

The approach involves a plot of $C_t/(C_0–C_t)$ vs. sampling time (t) according to Eq. (2). The parameters of k_{YN} and τ (the time required for 50% copper ion breakthrough) can be obtained using nonlinear regressive method. The values of k_{YN} and τ are listed in Table 2.

From Table 2, the rate constant k_{YN} increased and the 50% breakthrough time τ decreased with both increasing flow rate and copper ions influent concentration. With the bed depth increasing, the values of τ increased while the values of k_{YN} decreased. The data in Table 2 also indicated that values τ were similar to experimental results.

As Thomas model and Yoon–Nelson model can be transformed on form, the values of R^2 and x^2 listed in Tables 1 and 2 are same at same experimental condition, respectively.

3.5.3. Clark model

Clark model was based on the use of a mass-transfer concept in combination with the Freundlich isotherm [24]:

$$\frac{C_t}{C_0} = \left(\frac{1}{1 + Ae^{-rt}}\right)^{1/(n-1)} \quad (3)$$

From a plot of C_t/C_0 against t at a given bed height and flow rate using nonlinear regressive analysis, the values of A and r can be obtained.

Table 1
Thomas model parameters at different conditions

C_0 (mg L^{-1})	v (mL min^{-1})	Z (cm)	q_{exp} (mg g^{-1})	q_0 (mg g^{-1})	k_{Th} (mL min^{-1} mg^{-1})	R^2	x^2
NWS							
20	5.6	6.0	4.49	4.04	13.2	0.989	0.00095
20	5.6	8.5	4.36	3.38	9.82	0.969	0.00305
20	5.6	11.0	4.56	3.06	8.54	0.930	0.00725
20	3.6	8.5	5.24	4.14	9.4	0.980	0.00324
20	7.6	8.5	3.69	3.02	14.5	0.975	0.00201
10	5.6	8.5	3.18	2.62	19.06	0.973	0.00462
30	5.6	8.5	5.35	3.95	9.22	0.976	0.00237
MWS							
20	5.6	6.0	7.64	6.21	9.73	0.968	0.00446
20	5.6	8.5	7.16	6.05	7.90	0.978	0.00315
20	5.6	11.0	6.84	5.52	6.16	0.970	0.00459
20	3.6	8.5	7.88	6.78	6.31	0.985	0.00193
20	7.6	8.5	5.86	4.98	12.3	0.973	0.00441
10	5.6	8.5	6.48	4.92	8.22	0.956	0.00641
30	5.6	8.5	8.20	6.45	7.17	0.981	0.00270

Note: $x^2 = \sum (q - q_c)^2$, q and q_c are the experimental value and calculated value according the model, respectively.

In previous study, it was found that the Freundlich model was approximately valid for the adsorption of copper on NWS and MWS in batch adsorption [4,16], so the Freundlich constant $1/n$ (0.364 for NWS, 0.819 for MWS) obtained in batch experiment were used to calculate the parameters in the Clark model. The values of A and r in the Clark model are determined using Eq. (3) by nonlinear regression analysis and are shown in Table 3. From Table 3, as both flow rate and influent dye concentration increased, the values of r increased.

Compared values of R^2 and x^2 are listed in Tables 1 and 3 (or Table 2), value of R^2 from Thomas model (Yoon–Nelson model) is larger than that from Clark

Table 2
Yoon–Nelson parameters at different conditions

C_0 (mg L^{-1})	V (mL min^{-1})	Z (cm)	k_{YN}/(L min^{-1})	τ/min	τ_e/min	R^2	x^2
NWS							
20	5.6	6.0	0.293	9.14	8.6	0.989	0.0095
20	5.6	8.5	0.202	12.0	11.5	0.968	0.00305
20	5.6	11.0	0.172	14.8	13.6	0.930	0.00725
20	3.6	8.5	0.208	23.1	22.5	0.980	0.00324
20	7.6	8.5	0.320	7.99	7.2	0.976	0.00201
10	5.6	8.5	0.189	18.7	17.1	0.969	0.00466
30	5.6	8.5	0.277	9.69	8.6	0.975	0.00237
MWS							
20	5.6	6.0	0.199	15.6	14.4	0.968	0.00446
20	5.6	8.5	0.158	21.6	20.1	0.978	0.00315
20	5.6	11.0	0.123	25.5	24.4	0.970	0.00459
20	3.6	8.5	0.126	37.7	35.6	0.973	0.00441
20	7.6	8.5	0.245	13.1	12.5	0.985	0.00192
10	5.6	8.5	0.0817	35.2	33.6	0.951	0.00641
30	5.6	8.5	0.215	15.8	15.1	0.981	0.00270

Table 3
Clark parameters at different conditions

C_0 (mg L^{-1})	V (mL min^{-1})	Z (cm)	A	r	R^2	x^2
NWS						
20	5.6	6.0	4.64	0.250	0.991	0.00720
20	5.6	8.5	3.86	0.176	0.975	0.00241
20	5.6	11.0	4.25	0.148	0.940	0.00623
20	3.6	8.5	28.48	0.178	0.984	0.00258
20	7.6	8.5	4.29	0.277	0.981	0.00155
10	5.6	8.5	10.20	0.164	0.975	0.00368
30	5.6	8.5	4.74	0.238	0.981	0.00183
MWS						
20	5.6	6.0	1.97E5	0.566	0.939	0.00852
20	5.6	8.5	2.23E5	0.402	0.950	0.00755
20	5.6	11.0	1.64E5	0.335	0.937	0.00705
20	3.6	8.5	8.6E5	0.365	0.947	0.00884
20	7.6	8.5	1.91E5	0.659	0.968	0.00429
10	5.6	8.5	5.91E4	0.212	0.907	0.0122
30	5.6	8.5	3.97E5	0.598	0.960	0.00563

model while x^2 is smaller at same condition for NWS. But for MWS, they are opposite. Moreover, the difference is smaller. So the three models can be used to predict the breakthrough curves.

3.5.4. BDST model

The BDST model is based on physically measuring the capacity of the bed at different breakthrough values. The BDST model works well and provides useful modeling equations for the changes of system parameters [25]. A modified form of the equation that expresses the service time at breakthrough, t, as a fixed function of operation parameters is BDST model:

$$t = \frac{N_0}{C_0 F} Z - \frac{1}{K_a C_0} \ln\left(\frac{C_0}{C_t} - 1\right) \quad (4)$$

where C_t is the effluent concentration of solute in the liquid phase (mg L^{-1}); C_0 is the initial concentration of solute in the liquid phase (mg L^{-1}); F is the influent linear velocity (cm min^{-1}); N_0 is the adsorption quantity (mg L^{-1}); K_a is the rate constant in BDST model (L mg^{-1} min^{-1}); t is the time (min); and Z is the bed depth of column (cm).

A plot of t vs. bed depth, Z, should yield a straight line where N_0 and K, the adsorption capacity and rate constant, respectively, can be evaluated.

The lines of t–Z at values of C_t/C_0 0.2, 0.6, and 0.8 for NWS and MWS are shown in Fig. 6, respectively. The related constants of BDST according to the slopes and intercepts of lines are listed in Table 4.

From Table 4, it was shown that the value of N_0 increased dramatically while the rate constant of K_a increased along with the value of C_t/C_0 increasing. According to the values of R^2, the rationality of the BDST model was identified for the adsorption processes. Moreover, MWS had more excellent adsorption capacity along with higher values of N_0, compared with NWS in the same situation.

In addition, The BDST model constants can be used to predict the adsorbent performance for other flow rate and concentration without further process. A simplified form of the BDST model is:

Table 4
Calculated constants of the BDST model for the adsorption of copper ion onto NWS and MWS ($C_0 = 20$ mg L^{-1}, $v = 5.6$ mL min^{-1})

C_t/C_0	a (min cm^{-1})	b (min)	K_a (L mg^{-1} min^{-1})	N_0 (mg L^{-1})	R^2
NWS					
0.2	0.606	−0.978	7.09×10^{-4}	67.9	0.999
0.6	0.685	−6.67	3.04×10^{-3}	76.7	0.953
0.8	1.92	−3.46	2.00×10^{-2}	215	0.887
MWS					
0.2	1.13	−2.99	-2.32×10^{-2}	127	0.856
0.6	2.29	−2.42	8.37×10^{-3}	257	0.98
0.8	2.95	−7.52	9.22×10^{-3}	331	0.974

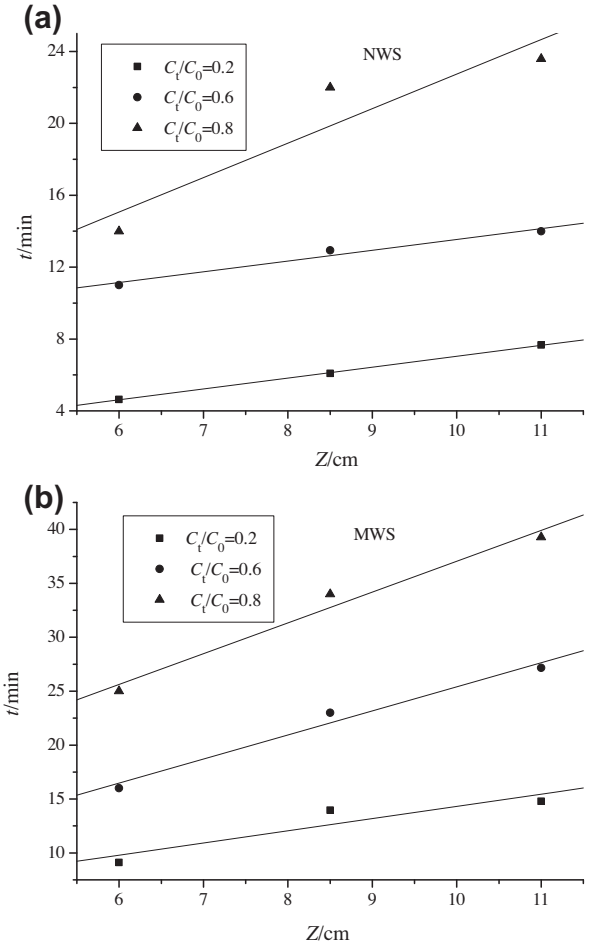

Fig. 6. Isoremoval lines for 0.2, 0.4, and 0.6 breakthrough for different bed depths ($C_0 = 20\,mg\,L^{-1}$, $v = 5.6\,mL\,min^{-1}$).

$$t = aZ - b \tag{5}$$

where

$$a = \frac{N_0}{C_0 F} \tag{6}$$

$$b = \frac{1}{K_a C_0} \ln\left(\frac{C_0}{C_t} - 1\right) \tag{7}$$

The slope constant for a different flow rate can be directly calculated by Eq. (6) [25]:

$$a' = a\frac{F}{F'} = a\frac{v}{v'} \tag{8}$$

where a and F are the old slope and influent linear velocity, respectively, and a' and F' are the new slope and influent linear velocity, respectively. As the column used in experiment has the same diameter, the ratio of original (F) and the new influent linear velocity (F') and original flow rate (v) and the new flow rate (v') is equal.

For other influent concentrations, the desired equation is given by a new slope, and a new intercept is given by

$$a' = a\,\frac{C_0}{C_0'} \tag{9}$$

$$b' = b \cdot \frac{C_0}{C_0'} \cdot \frac{\ln(C_0'/C_f' - 1)}{\ln(C_0/C_f - 1)} \tag{10}$$

where b' and b are the new and old intercepts, respectively; C_0' and C_0 are the new and old influent concentrations, respectively. C_f' is the effluent concentration at influent concentration C_0' and C_f is the effluent concentration at influent concentration C_0.

The BDST constants gained at flow rate $5.6\,mL\,min^{-1}$ and influent concentration $20\,mg\,L^{-1}$ was helpful to predict the column behavior at higher flow rate of $7.6\,mL\,min^{-1}$ and lower influent concentration of $10\,mg\,L^{-1}$, respectively. Meanwhile, the related calculated time (t_c) and experimental time (t_e) are listed in Tables 5 and 6, respectively.

In addition, The BDST model constants can be used to predict the adsorbent performance for other flow rate and concentration without further process. For instance, the BDST constants gained at flow rate $5.6\,mL\,min^{-1}$ and influent concentration $80\,mg\,L^{-1}$ were helpful to forecast the adsorbent behavior at higher flow rate of $7.6\,mL\,min^{-1}$ and lower influent concentration of $10\,mg\,L^{-1}$, respectively. Meanwhile, the corresponding calculated time (t_c) and experimental time (t_e) are demonstrated in Tables 5 and 6, respectively.

It was shown that some values of t_c were close to values of t_e while some were not, which indicated available prediction for the case of changed influent concentration and flow rate.

3.5.5. Theoretical breakthrough curve

The data obtained from the batch adsorption isotherm can be used to predict the theoretical breakthrough curve, which can be compared with the experimental curve. The detailed calculations for the generation of the experimental breakthrough curve from the equilibrium data obtained from batch studies are as follows [26]:

(1) An experimental equilibrium curve was plotted assuming various values of C_e (the value was equal to C_t) and calculating the corresponding

Table 5
Predicted breakthrough time based on the BDST constants for a new flow rate

C_t/C_0	V (mL min^{-1})	V' (mL min^{-1})	a' (min cm^{-1})	b' (min)	t_c (min)	t_e/min
NWS ($C_0 = 20$ mg L^{-1}, $Z = 8.5$ cm)						
0.2	5.6	7.6	0.447	−0.978	4.77	4.21
0.6	5.6	7.6	0.505	−6.67	11.0	8.72
0.8	5.6	7.6	1.42	−3.46	15.5	13.5
MWS ($C_0 = 20$ mg L^{-1}, $Z = 8.5$ cm)						
0.2	5.6	7.6	0.835	−2.99	10.1	7.93
0.6	5.6	7.6	1.69	−2.42	16.8	14.7
0.8	5.6	7.6	2.17	−7.52	26.0	19.5

Table 6
Predicted breakthrough time based on the BDST constants for a new copper ion concentration

C_t/C_0	C_0 (mg L^{-1})	C_0' (mg L^{-1})	a' (min cm^{-1})	b' (min)	t_c (min)	t_e (min)
NWS ($v = 5.6$ mL min^{-1}, $Z = 8.5$ cm)						
0.2	20	10	1.21	−1.96	12.3	12.4
0.6	20	10	1.37	−13.4	25.0	19.0
0.8	20	10	3.84	−6.93	39.6	29.9
MWS ($v = 5.6$ mL min^{-1}, $Z = 8.5$ cm)						
0.2	20	10	2.27	−5.98	25.2	19.5
0.6	20	10	4.59	−4.84	43.8	37.2
0.8	20	10	5.90	−15.0	65.2	60.6

values of q_e using the best fit isotherm model obtained from the batch adsorption results.

(2) An operating line was drawn, which was through the original and end points obtained by experimental equilibrium curve. The significance of this operating line is that the data of the continuously batch reactor and the data of the fixed-bed reactor are identical at these two points, first at the initiation and other at the exhaustion of the reaction.

(3) The rate of transfer of solute from solution over a differential depth of column, dh, is given by

$$vdC = K_m(C - C^*)dh \tag{11}$$

where v is the wastewater flow rate, K_m is the overall mass transfer coefficient, which includes the resistances offered by film diffusion and pore diffusion and C^* is the equilibrium concentration of solute in solution corresponding to an adsorbed concentration, q_e.

The term $C - C^*$ is the driving force for adsorption and is equal to the distance between the operating line and equilibrium curve at any given value of q_e. Integrating Eq. (10) and solving for the height of the adsorption zone,

$$h_Z = \frac{v}{K_m}\int_{C_B}^{C_E}\frac{dC}{C - C^*} \tag{12}$$

For any value of h less than h_z, corresponding to a concentration C between C_B and C_E, Eq. (12) can be written

$$h = \frac{v}{K_m}\int_{C_B}^{C}\frac{dC}{C - C^*} \tag{13}$$

Dividing Eq. (13) by Eq. (12) results in

$$\frac{h}{h_z} = \frac{\int_{C_B}^{C} dC/(C - C^*)}{\int_{C_B}^{C_E} dC/(C - C^*)} = \frac{V - V_B}{V_E - V_B} \tag{14}$$

where V_B and V_E are total volume of water treated till breakthrough and up to exhaust point, respectively, and V is the volume of

water treated within V_E for effluent concentration C with in C_E. Dividing the values of $\int_{C_B}^{C} dC/(C - C^*)$ by the value of $\int_{C_B}^{C_E} dC/(C - C^*)$ the term $(V-V_B)/(V_E-V_B)$ was evaluated.

(4) Now the plot of $C/C0$ vs. $(V-V_B)/(V_E-V_B)$ represents the theoretical breakthrough curve.

Evaluating the result from fitting the batch experimental data, it was showed that Langmuir isotherm provided a best fitness [4,16]. So the Langmuir isotherm was used to generate the theoretical breakthrough curve. Fig. 7 showed the theoretical breakthrough curve compared with the experimental breakthrough curve which relevant to 8.5 cm bed depth and initial copper ion concentration of $20\,mg\,L^{-1}$ with flow rate $5.6\,mL\,min^{-1}$. For NWS, the two curves followed the same trend with small differences. But for MWS, the two curves followed same trend and there were some difference. Therefore, Langmuir isotherm constants found from the batch experimental data can be used to predict the breakthrough in fixed-bed system for copper ion adsorption onto NWS.

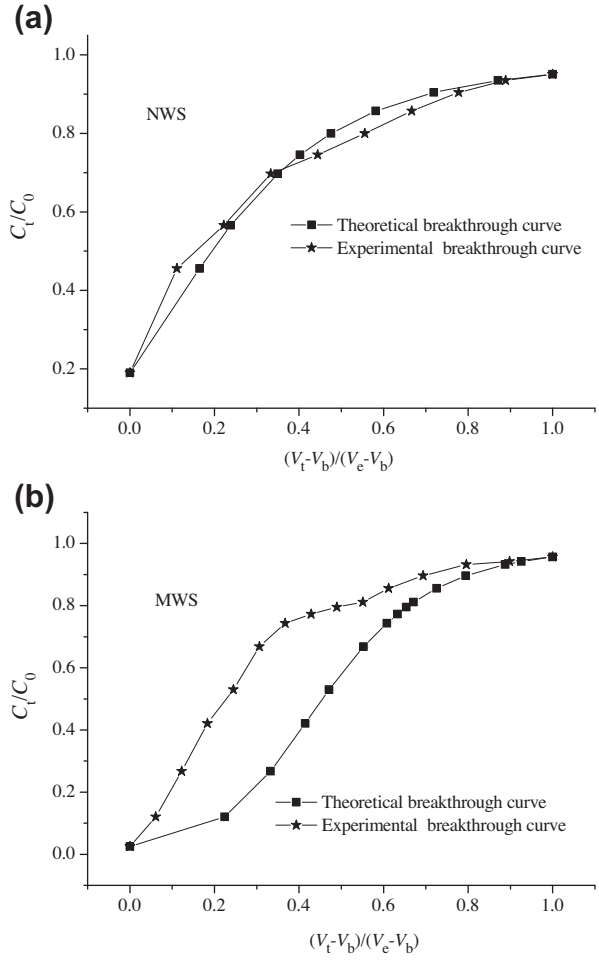

Fig. 7. Theoretical and experimental breakthrough curve of copper adsorption in column mode.

4. Conclusion

This study showed that NWS and MWS was an effective adsorbent for removal of copper ion from aqueous solution. The adsorption of copper ion was strongly dependent on the flow rate, the initial copper ion concentration, and bed depth. The breakthrough process can be fitted by Thomas and the breakthrough data predictions by BDST model showed some agreement with experiment data. The mass transfer model could provide a good agreement between the experimental breakthrough curve and the theoretical breakthrough curve. Copper ion was easily desorbed from NWS and MWS column using $0.5\,mol\,L^{-1}$ HCl solution and the NWS and MWS column can be reused to remove copper ion from aqueous solution efficiently.

Acknowledgment

This work was supported by the National Natural Science Foundation of China for undergraduate cultivation in basic science (J1210060).

References

[1] V.K. Gupta, Suhas Application of low-cost adsorbents for dye removal – A review, J. Environ. Manage. 90(8) (2009) 2313–2342.
[2] V.K. Gupta, P.J.M. Carrott, M.M.L. Ribeiro Carrott, Suhas Low cost adsorbents: Growing approach to wastewater treatment – A review, Crit. Rev. Env. Sci. Technol. 39 (2009) 783–842.
[3] C.R. Teixeira Tarley, M.A. Zezzi Arruda, Biosorption of heavy metals using rice milling by-products. Characterisation and application for removal of metals from aqueous effluents, Chemosphere 54 (2004) 987–995.
[4] Y.J. Wu, L.J. Zhang, C.L. Gao, J.Y. Ma, X.H. Ma, R.P. Han, Adsorption of copper ions and methylene blue in single and binary system on wheat straw, J. Chem. Eng. Data 54 (2009) 3229–3234.
[5] V.B.H. Dang, H.D. Doan, T. Dang-Vuc, A. Lohi, Equilibrium and kinetics of biosorption of cadmium(II) and copper(II) ions by wheat straw, Bioresour. Technol. 100 (2009) 211–219.
[6] R.P. Han, J.H. Zhang, W.H. Zou, J. Shi, H.M. Liu, Equilibrium biosorption isotherm for lead ion on chaff, J. Hazard. Mater. 125 (2005) 266–271.
[7] G. McKay, Y.S. Ho, J.C.P. Ng, Biosorption of copper from waste waters: A review, Sep. Purif. Methods 2 (1999) 87–125.
[8] M. Gavrilescu, Removal of heavy metals from environment by biosorption, Eng. Life Sci. 4 (2004) 219–232.
[9] T.G. Chuah, A. Jumasiah, I. Azni, S. Katayon, S.Y. Thomas Choong, Rice husk as a potentially low-cost biosorbent for heavy metal and dye removal: An overview, Desalination 175 (2005) 305–316.
[10] J. Febrianto, A.N. Kosasih, J. Sunarso, Y.H. Ju, N. Indraswati, S. Ismadji, Equilibrium and kinetic studies in adsorption of heavy metals using biosorbent: A summary of recent studies, J. Hazard. Mater. 162 (2009) 616–645.

[11] W.S. Wan Ngah, M.A.K.M. Hanafiah, Removal of heavy metal ions from wastewater by chemically modified plant wastes as adsorbents: A review, Bioresour. Technol. 99 (2008) 3935–3948.
[12] D.W. O'Connell, C. Birkinshaw, T.F. O'Dwyer, Heavy metal adsorbents prepared from the modification of cellulose: A review, Bioresour. Technol. 99 (2008) 6709–6724.
[13] H.P. Ye, Q. Zhu, D.Y. Du, Adsorptive removal of Cd(II) from aqueous solution using natural and modified rice husk, Bioresour. Technol. 101 (2010) 5175–5179.
[14] Z.W. Wang, P. Han, Y.B. Jiao, X.T. He, C.C. Dou, R.P. Han, Adsorption of congo red using ethylenediamine modified wheat straw, Desalin. Water Treat. 30 (2011) 195–206.
[15] U. Kumar, M. Bandyopadhyay, Fixed bed column study for Cd(II) removal from wastewater using treated rice husk, J. Hazard. Mater. 129 (2006) 253–259.
[16] R.P. Han, L.J. Zhang, C. Song, M.M. Zhang, H.M. Zhu, L.J. Zhang, Characterization of modified wheat straw, kinetic and equilibrium study about copper ion and methylene blue adsorption in batch mode, Carbohydr. Polym. 79 (2010) 1140–1149.
[17] W.E. Marshall, L.H. Wartelle, D.E. Boler, M.M. Johns, C.A. Toles, Enhanced metal adsorption by soybean hulls modified with citric acid, Bioresour. Technol. 69 (1999) 263–268.
[18] R.P. Han, J.H. Zhang, W.H. Zou, H.J. Xiao, J. Shi, H.M. Liu, Biosorption of copper(II) and lead(II) from aqueous solution by chaff in a fixed-bed column, J. Hazard. Mater. 133 (2006) 262–268.
[19] A. Mittal, J. Mittal, A. Malviya, D. Kaur, V.K. Gupta, Decoloration treatment of a hazardous triarylmethane dye, light green SF (yellowish) by waste material adsorbents, J. Colloid Interface Sci. 342 (2010) 518–527.
[20] V.K. Gupta, I. Ali, Utilisation of bagasse fly ash (a sugar industry waste) for the removal of copper and zinc from wastewater, Sep. Purif. Technol. 18 (2000) 131–140.
[21] A. Mittal, J. Mittal, A. Malviya, D. Kaur, V.K. Gupta, Adsorption of hazardous dye crystal violet from wastewater by waste materials, J. Colloid Interface Sci. 343 (2010) 463–473.
[22] Z. Aksu, F. Gonen, Biosorption of phenol by immobilized activated sludge in a continuous packed bed: Prediction of breakthrough curves, Process Biochem. 39 (2004) 599–613.
[23] Y.H. Yoon, J.H. Nelson, Application of gas adsorption kinetics. I. A theoretical model for respirator cartridge service time, Am. Ind. Hyg. Assoc. J. 45 (1984) 509–516.
[24] R.M. Clark, Evaluating the cost and performance of field-scale granular activated carbon systems, Environ. Sci. Technol. 21 (1987) 573–580.
[25] J. Goel, K. Kadirvelu, C. Rajagopal, V.K. Garg, Removal of lead(II) by adsorption using treated granular activated carbon: Batch and column studies, J. Hazard. Mater. 125 (2005) 211–220.
[26] S.K. Maji, A. Pal, T. Pal, A. Adak, Modeling and fixed bed column adsorption of As(III) on laterite soil, Sep. Purif. Technol. 56 (2007) 284–290.